Supplement of Atmos. Meas. Tech., 19, 7421–7444, 2026
https://doi.org/10.5194/amt-19-7421-2026-supplement
© Author(s) 2026. CC BY 4.0 License.



Atmospheric Measurement Techniques
Open Access
EGU

Supplement of

An incoherent broadband cavity-enhanced absorption spectrometer for simultaneous NO_3 and N_2O_5 measurements, integrated into a NO_y instrument suite: characterization and first field deployment

Patrick Dewald et al.

Correspondence to: Patrick Dewald (patrick.dewald@lisa.ipsl.fr) and Manuela Cirtog (manuela.cirtog@lisa.ipsl.fr)

The copyright of individual parts of the supplement might differ from the article licence.

Supplement

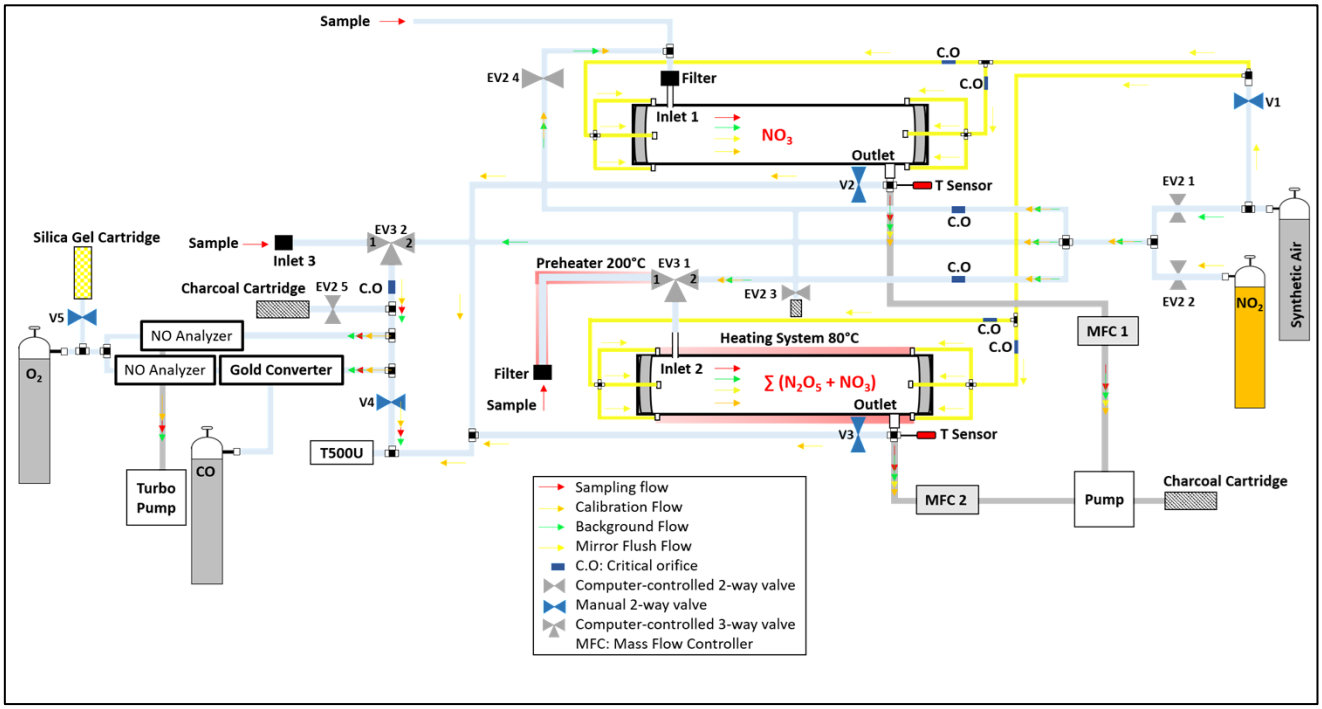


Figure S1. Detailed schematic diagram of the NOyBOx instrument and its flow system.

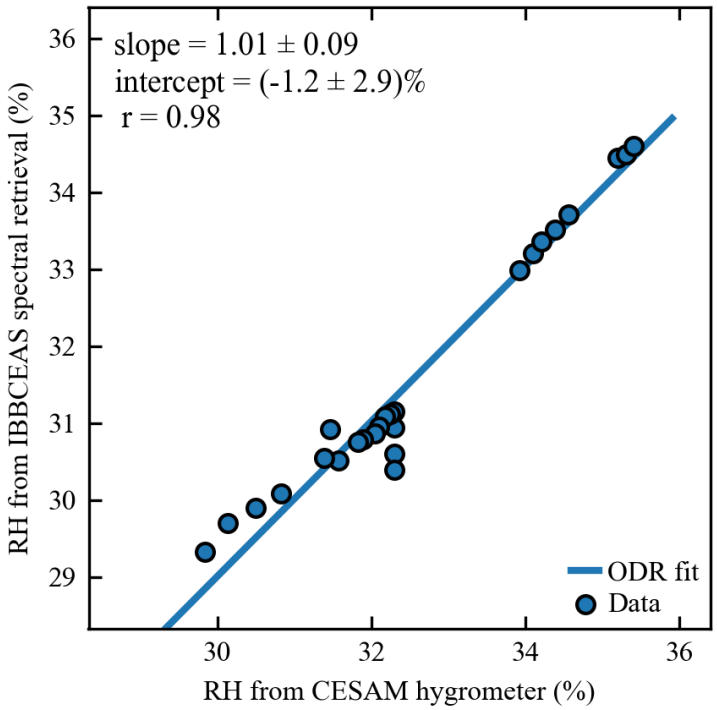


Figure S2. Relative humidity (RH) retrieved from the IBBCEAS spectra compared with the RH measured by the hygrometer of the CESAM chamber. The solid line is an orthogonal distance regression (ODR) of the IBBCEAS-retrieved RH on the hygrometer RH. The fit gives a slope of 1.01 ± 0.09 and an intercept of (−1.2 ± 2.9) %RH, where the uncertainties are two standard errors; the Pearson correlation coefficient is $r = 0.98$. The slope is consistent with unity within the fit uncertainty, and the IBBCEAS retrieval is on average 1 %RH lower than the hygrometer over the sampled range (about 30–35 %RH).

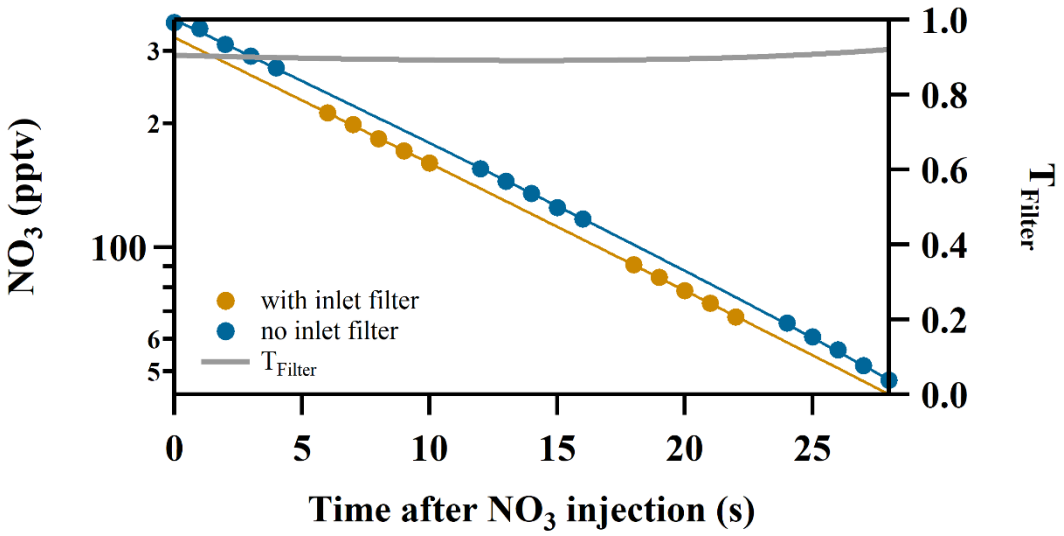


Figure S3. Decay of NO_3 as a function of time after NO_3 injection into the CESAM chamber, sampled with (orange) and without (blue) the inlet filter installed. Solid lines represent exponential fits to the respective decay curves. The filter transmission (T_{Filter}, grey, right axis), calculated as the ratio of the two fitted decays, remained close to 0.9 throughout the measurement.

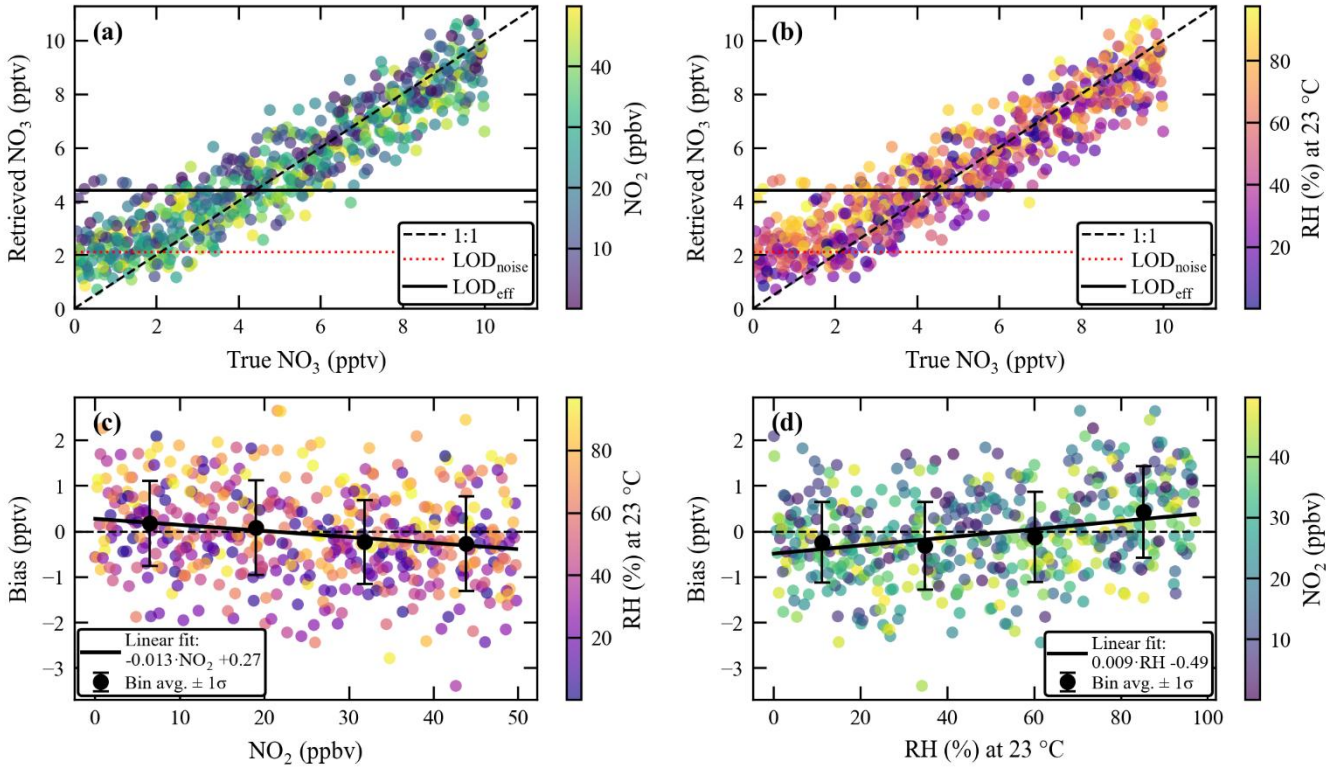


Figure S4. Retrieval performance of the NO_3 fitting routine as a function of interfering NO_2 and water vapor, based on Monte Carlo simulations of synthetic spectra for the N_2O_5 channel (10 noise realisation points average, 600 LHS points): (a, b) Retrieved vs. true NO_3 mixing ratio, with points colored by (a) true NO_2 (ppbv) and (b) relative humidity (RH, % at 23°C). The dashed line indicates the 1:1 relationship; the dotted red line marks LOD_{noise} derived from the Allan deviation, and the solid black line marks the effective detection limit LOD_{eff}, which additionally incorporates the standard deviation (2σ) of the retrieval bias across all simulated spectra. (c, d) Retrieval bias (retrieved − true NO_3) for points $NO_3 > LOD_{noise}$ plotted against (c) NO_2 and (d) RH, colored by the complementary variable in each case. Black circles show bin-averaged values (± 1σ). Black lines show weighted linear fits to the bin-averaged points.

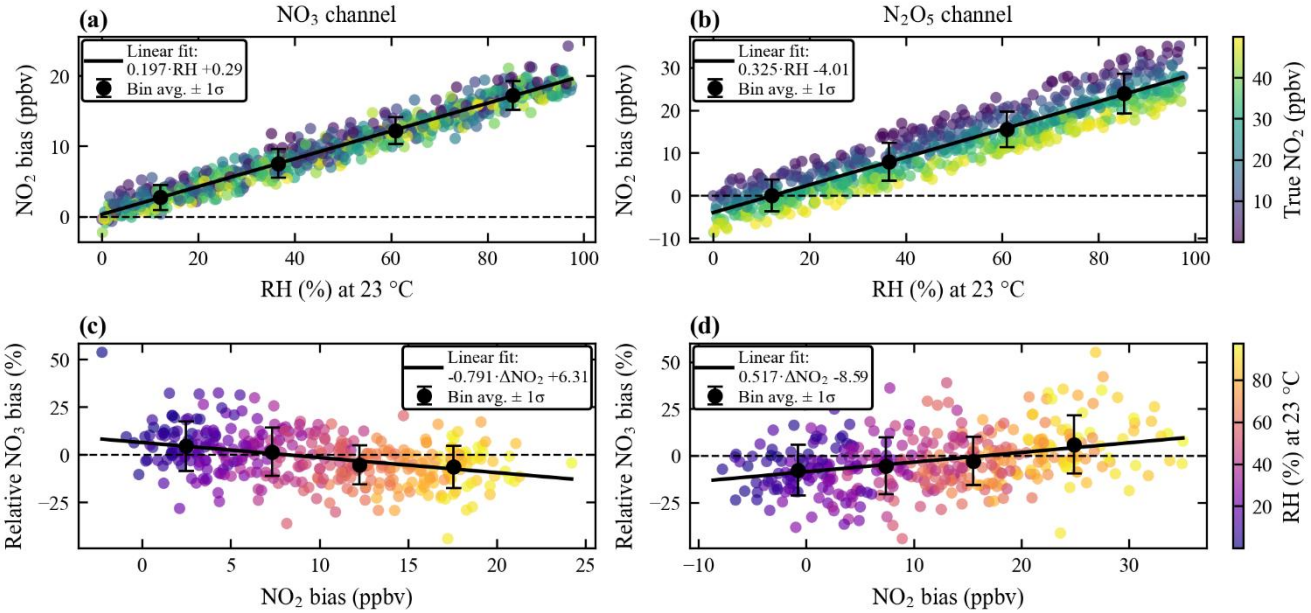


Figure S5. Systematic NO_2 retrieval bias and its effect on the retrieved NO_3 for the NO_3 cavity (left; a, c) and the N_2O_5 cavity (right; b, d), based on Latin hypercube–sampled synthetic spectra (N = 600 sampled points, each averaged over 10 Monte Carlo noise realisations, so the biases shown are systematic and less random). (a, b) Absolute NO_2 bias (retrieved − true, ppbv) as a function of relative humidity at 23 °C, coloured by the true NO_2 mixing ratio. (c, d) Relative NO_3 bias (%) as a function of the NO_2 bias (ppbv), coloured by relative humidity; only points with a true NO_3 above the noise-based limit of detection are shown, because the relative bias diverges for small NO_3. Black circles with error bars denote bin averages (four quantile bins) ± 1σ of the within-bin scatter, solid black lines are linear fits through the bin averages (parameters given in the legends), and dashed lines mark zero bias. Colour scales are identical for both cavities. In both cavities, the NO_2 bias increases with RH; in the N_2O_5 cavity it is additionally larger at low NO_2. Over the sampled NO_2 (0–50 ppbv) and RH (0–100 %) ranges, this NO_2 bias is weakly correlated to the retrieved NO_3, with Pearson correlation coefficients of –0.32 and +0.34 in the NO_3 and N_2O_5 cavities, respectively.

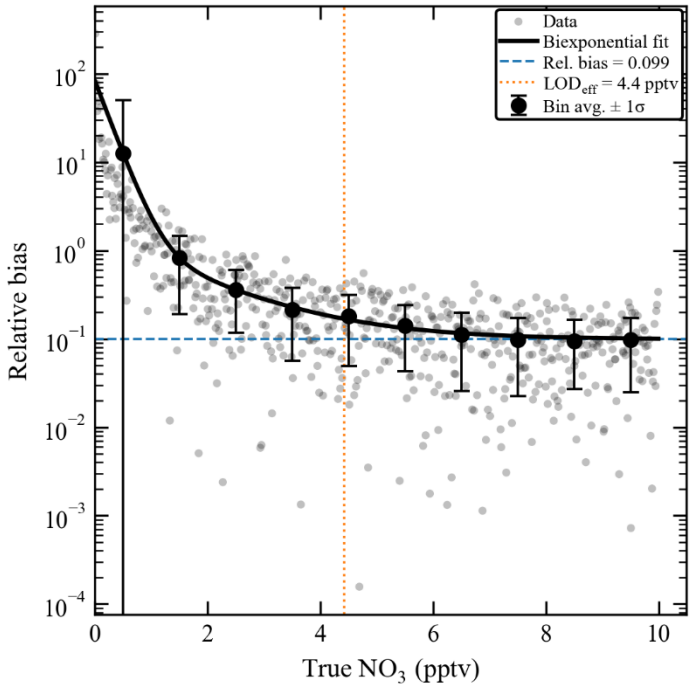


Figure S6. Relative bias in retrieved NO_3 (|retrieved − true| / true) versus true NO_3 concentration from Monte Carlo simulations for the N_2O_5 channel. Gray points: individual retrievals; black circles: quantile-binned means ± 1σ. Solid line: biexponential fit with parameters (a_1, a_2, b_1, b_2, c), relative bias = a_1 x exp(−b_1 x NO_3) + a_2 x exp(−b_2 x NO_3) + c, capturing the noise-dominated divergence at low NO_3 and the systematic interference floor (c = 0.099, blue dashed line) at higher NO_3. Orange dotted line: effective LOD.

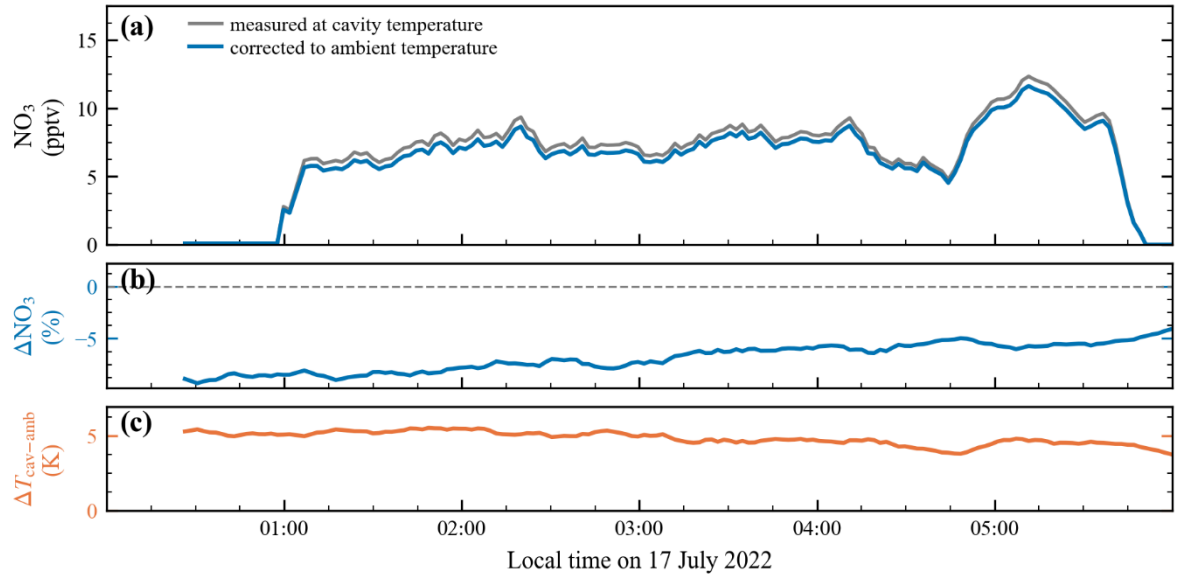


Figure S7. Correction of the measured NO_3 mixing ratio for the thermal shift of the NO_3–NO_2–N_2O_5 equilibrium in the cavity, for the night of 17 July 2022 (00:00–06:00 LT). (a) NO_3 as measured at cavity temperature (grey) and after correction to ambient temperature (blue). (b) Relative alteration of NO_3 caused by the correction, $\Delta NO_3 = (NO_{3,corr} - NO_{3,meas}) / NO_{3,meas}$. (c) Gas temperature difference between the cavity and ambient air (40 m), $\Delta T = T_{cav} - T_{amb}$. The correction factor was obtained using the box model used in section 3.3 for each data point by explicitly simulating the NO_3/N_2O_5 kinetics along the sampling line, starting from ambient equilibrium. The gas was assumed to be at ambient temperature until it entered the cavity, where it immediately reaches cavity temperature (residence time 1.3 s, pressure 970 mbar). It included an NO_3 wall loss of 0.1 s^{-1} in the cavity and a filter transmission of 0.9 for NO_3.